RSC Advances

ROYAL SOCIETY OF CHEMISTRY

www.rsc.org/advances

A new high sensitive phosphor for carbon ion dosimetry

Bhushan P. Kore[1], N.S.Dhoble[2], S.P. Lochab[3], S.J.Dhoble[1#]

[1]Department of Physics, RTM Nagpur University, Nagpur-440033, India
[2]Department of Chemistry, Sevadal Mahila Mahavidyalaya, Nagpur -440009, India
[3]Inter-University Accelerator Center, Aruna Asaf Ali Marg, New Delhi-110067, India

Abstract

Dy^{3+} doped $CaMg_3(SO_4)_4$ (CMS) phosphor was prepared by acid distillation method and its thermoluminescence (TL) study was carried out in detail. For TL study the phosphor was irradiated with γ-rays and carbon ion beam. Good dosimetric glow curve was observed which is stable against both the type of radiations. The CMS doped with 0.2mol% of Dy^{3+} shows 3.5 times more sensitivity than commercially available $CaSO_4:Dy^{3+}$ TLD phosphor, when irradiated with carbon ion beam. The observed glow curve variation and resultant variation in values of trapping parameters with change in ion beam energy suggest the more complex interactions of ion beam within phosphor at higher energies.

Keywords: Thermoluminescence, ion beam irradiation, TL kinetics, dosimetry.

I. INTRODUCTION

The demand for dosimetry of charged particle beams has taken decisive lead because of its utility in cancer diagnosis and therapy [1,2,3]. Ion beam therapy is found to be a crucial tool in clinical practice to cure the tumors in comparison to the conventional radiation beams [4,5]. The basis of this ion beam therapy is on the phenomenon of dose deposition at the Bragg's peak. In comparison to conventional radiation therapy such as γ- rays and high energy photon beams, heavy charge ion therapy is superior. Since the heavy charge particles (HCP) like C^{5+} ions are heavier than constituent particles in conventional radiations, which ensures the penetration into the final treatment locations deep inside the body with minimum scattering and stiffer particle trajectories, low straggling effects and sharper field edges [4]. The ion beam therapies appear to be a more favorable option than conventional photon therapy. The ion beam therapy has several advantages over photon therapy. Ion beams have well defined range and small angular scattering compared with conventional photon or electron beam radiotherapy. Conventional photon beam has a limited depth of penetration proportional to the energy of the accelerator. Beams of protons and carbon ions have a much more favorable dose-depth distribution than photons and are the new frontiers of cancer radiation therapy [5]. Heavy ion beams deliver a larger mean energy per unit length of their

trajectory in the body than proton and photon beams [6]. The bone and soft-tissue tumors are usually operated with surgery because such type of tissues are generally radio-resistant and the effect of photon radiation is not sufficient for long term control but when surgical operations are difficult to perform radiotherapy is often employed as a sole treatment. In this sense carbon ion radiotherapy shows higher biological effects than others [7]. These factors are very crucial for tumors located close to critical organs like eye, ear etc. Tumors are to be treated with appropriate higher dose with special care that healthy tissues are not influenced by the incident ion beam. This opens up a promising potential for their highly effective use in the treatment of intractable cancers. For this the diagnosis and therapy of dose delivered to tumor requires accurate calibration of radiotherapy sources and their proper dosimetry. These ideas encourage us to find a suitable TLD phosphor for carbon ion dosimetry. For high energies of heavy charged particles in the entrance region low ionization density commonly produces repairable damages. But with increased energy, energy loss towards the Bragg Peak is more significant which produces irreparable damages giving a higher relative biological efficiency (RBE). Biological effectiveness refers to the difference in rate at which cells are killed with the same radiation dose. We have selected carbon ion for study because heavier and lighter ions possess their own drawbacks. The limitations of using heavier ions like neon or argon is that they causes irreparable damages in the entrance channel (surface) and thus significantly damaging the healthy tissues in front of the tumor [8]. For very light ions like protons the scattering effect is large and therefore no damage potentiation (the increase in strength of nerve impulses along pathways which have been used previously) can be observed in the target volume [8]. Hence, carbon ion beams represent a most favorable option in heavy ion therapy and for enhancing the biological efficiency in tumor therapy [9].

Sulphate based TL materials are known for their high sensitive TL response. It has been found that mixed sulfates form a class of TL phosphors with good TL characteristic, when doped with appropriate activators [10-13]. This family includes several materials such as $CaSO_4:Dy^{3+}$, $K_2Ca_2(SO_4)_3$:Eu, $LiNaSO_4$:Eu, $Na_{21}Mg(SO_4)_{10}Cl_3:Dy^{3+}$, $K_3Na(SO_4)_2$:Eu, etc., which are studied due to their excellent thermoluminescent properties such as high TL sensitivity, high TL efficiency, linear dose response over wide range of doses and reproducibility. But all these phosphors suffer from one or the other problem. More work is going on either to improve TL properties of these existing materials or to develop new high sensitive TL phosphors with ideal TL characteristic. Therefore, there is a great demand of highly efficient dosimetry materials for radiation dose assessment and to meet technological

challenges. Such efforts are also crucial in a number of other areas like extended human presence in outer space [14]. Several methods and treatments have been adopted 1) to improve their TL sensitivity, 2) to know the responsible defects in these materials and 3) to understand the phenomenon of TL in more detail.

To the best of our knowledge, the literature on the effect of carbon ion beams on phosphor materials especially with reference to dosimetry is very limited. This study is an attempt to bring out some useful results on the TL response of carbon beam irradiated high sensitive phosphor, which would be helpful in dosimetry of carbon ion beam.

II. EXPERIMENTAL

A. Synthesis method

The phosphor studied in present work was synthesized using method described by Yamashita *et al* [15]. For the preparation of CMS phosphor all the starting materials used were of analytical grade. CMS doped with different concentration of Dy^{3+} was prepared by dissolving $CaSO_4$, $MgSO_4$ and stoichiometric amount Dy_2O_3 in 15ml of hot sulfuric acid (the excess acid used). The mixture was allowed to heat at about 300 °C for 20hrs, during heating the acid vapors were condensed using condenser assembly through which the cool water is flowing continuously. The purpose of condensing the acid vapors is to avoid the accident arising from these highly reactive vapors. After cooling the mixture to room temperature excess acid present in sample is washed out repeatedly with distilled water and water insoluble compound was obtained which is in the form of small crystals. After washing the samples 4 to 5 times with distilled water the remaining sample was dried in oven at 80 °C. No further heat treatment was given to the samples.

B. Experimental Details

FIG. 1 (a), (b) Copper ladder with pellets of CMS sample mounted on it, (c) inner view of C^{5+} ion irradiation chamber.

5mg of CMS phosphor was exposed to γ-rays from ^{60}Co and ^{137}Cs sources for various doses to see the glow curve structure variation with dose and linearity of the phosphor. The samples in the form of pellets were irradiated at room temperature by C^{5+} ion beam at energies of 50MeV and 75MeV for different ion fluences in the range 15×10^{10} to 30×10^{12} ions/cm^2, using a 16MV Tandem Van de Graff type electrostatic accelerator (15UD pelletron) at the Inter-University Accelerator Center, New Delhi, India. The full details of this set up are given by Kanjilal *et al.*[16]. For irradiation the pellets of sample were mounted on a copper target ladder, as shown in Fig.1 (a) and (b). The copper ladder prevents heating of sample during Swift Heavy Ion (SHI) irradiation. For irradiation the ladder was kept inside the evacuated irradiation chamber, shown in Fig.1 (c). The ion beams were magnetically scanned on a 10mm x10mm area of sample surfaces for a uniform irradiation. The beam spot size used was 2.5 mm^2. The pressure of vacuum chamber during ion beam irradiation is 5×10^{-4} mbar.

The diffraction pattern of the CMS phosphor was examined using synchrotron XRD (SXRD) measurements at ADXRD beamline (BL-12) of Indus-2 synchrotron source, RRCAT, Indore, India [17, 18]. Image plate area detector (Mar 345 Dtb) was used to record the diffraction pattern. Lanthanum hexaborate (LaB_6) was used as a standard material for calibration of the beam energy and the sample to detector distance. The wave-length used was 0.77774Å. The TL glow curves were recorded using a Harshaw TLD reader (Model 3500) fitted with 931B PMT. The heating rate used was 5°C/s. The photoluminescence (PL) emission spectra of the samples were recorded by using a RF-5301PC SHIMADZU Spectrofluorophotometer. Emission and excitation spectra were recorded using a spectral slit width of 1.5nm.

III. RESULT AND DISCUSSION

A. X-ray diffraction

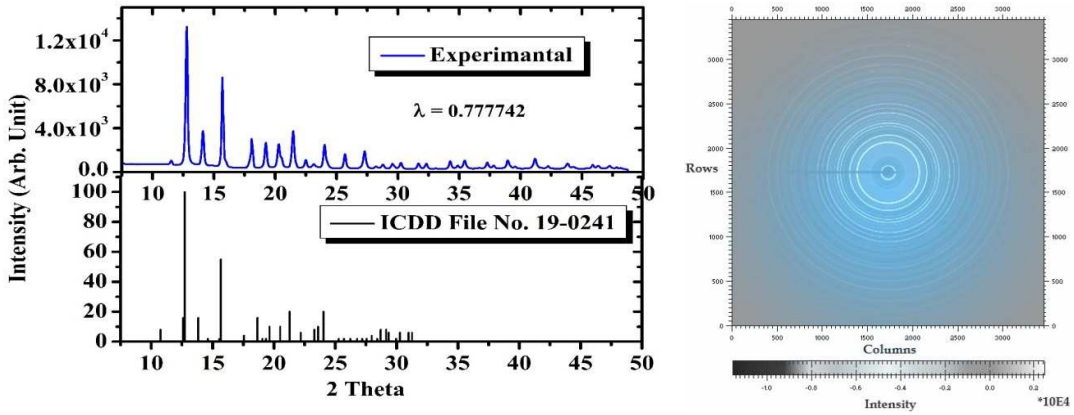

FIG. 2(a) High-resolution synchrotron X-ray diffraction patterns of CMS phosphor, (b) the raw image plate x-ray diffraction data.

X-ray diffraction pattern of CMS phosphor was recorded using the beam energy of 15.94keV and by keeping sample to image plate distance as 151.2mm (refined values using FIT2D). The image plate data files were integrated using software FIT2D, incorporating polarization correction [19]. To know more in detail about the phase of this phosphor the high resolution synchrotron X-ray diffraction data collected at room temperature, as shown in Fig. 2. Angle dispersive synchrotron XRD pattern are nearly pure phase and in good agreement with the standard ICDD File No.19-0241. The different Dy^{3+} concentration doped XRD pattern of CMS phosphor is shown in Fig. (S1), see supplementary material [20]. All the four XRD patterns are almost identical which suggest that the incorporation of Dy^{3+} into the CMS lattice does not influence the crystal structure. Fig. (S2) shows the modification in the XRD pattern of this phosphor after C^{5+} ion beam irradiation. The video illustrating the ion beam irradiation on sample's pellets is also given in supplementary information, see file M1. No new peaks were observed after ion beam irradiation indicating no change in phase of phosphor. Due to ion beam irradiation the relative intensities of some dominant peaks changes and some minor peaks are diminished. This alteration is small indicating small reduction in the crystallinity of the phosphor after ion beam irradiation. Therefore, we can say that this phosphor is stable against the C^{5+} ion beam irradiation.

B. SEM Study

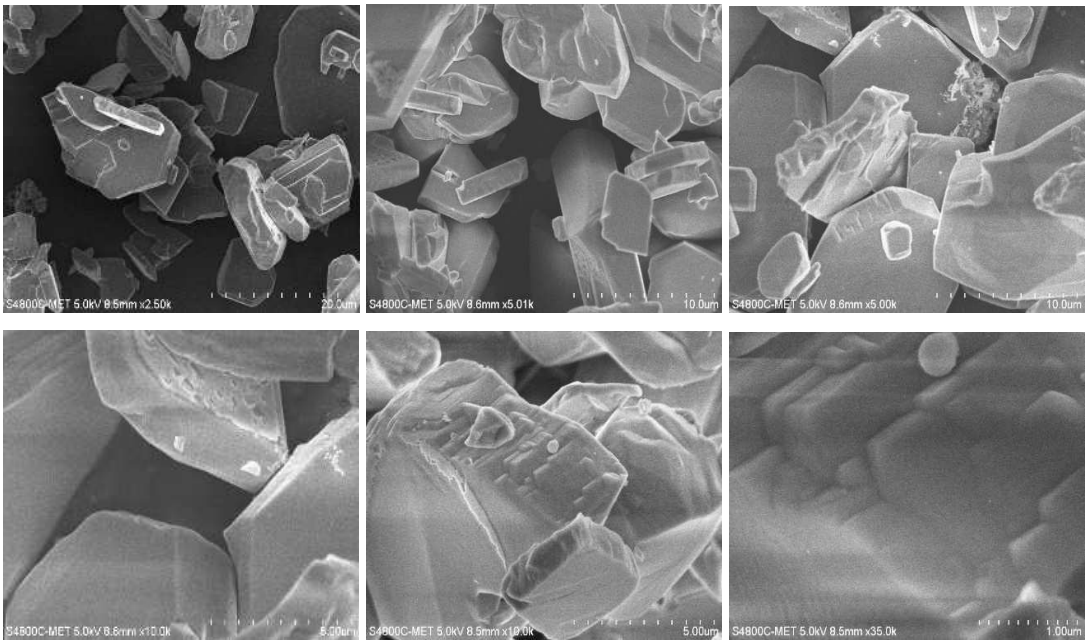

FIG. 3 SEM images of CMS phosphor prepared by acid distillation method.

The SEM images of the as-synthesized samples are shown in Fig. 3. The large particles were formed when prepared by acid distillation method, some grains having disk shape and others are of irregular shape with fine surfaces. Figure shows the microstructures consist of large particles having size between 5 and 15μm range. This particle range is suitable for phosphor to be useful in dosimetry application [21].

C. TL study

1. Effect of irradiation

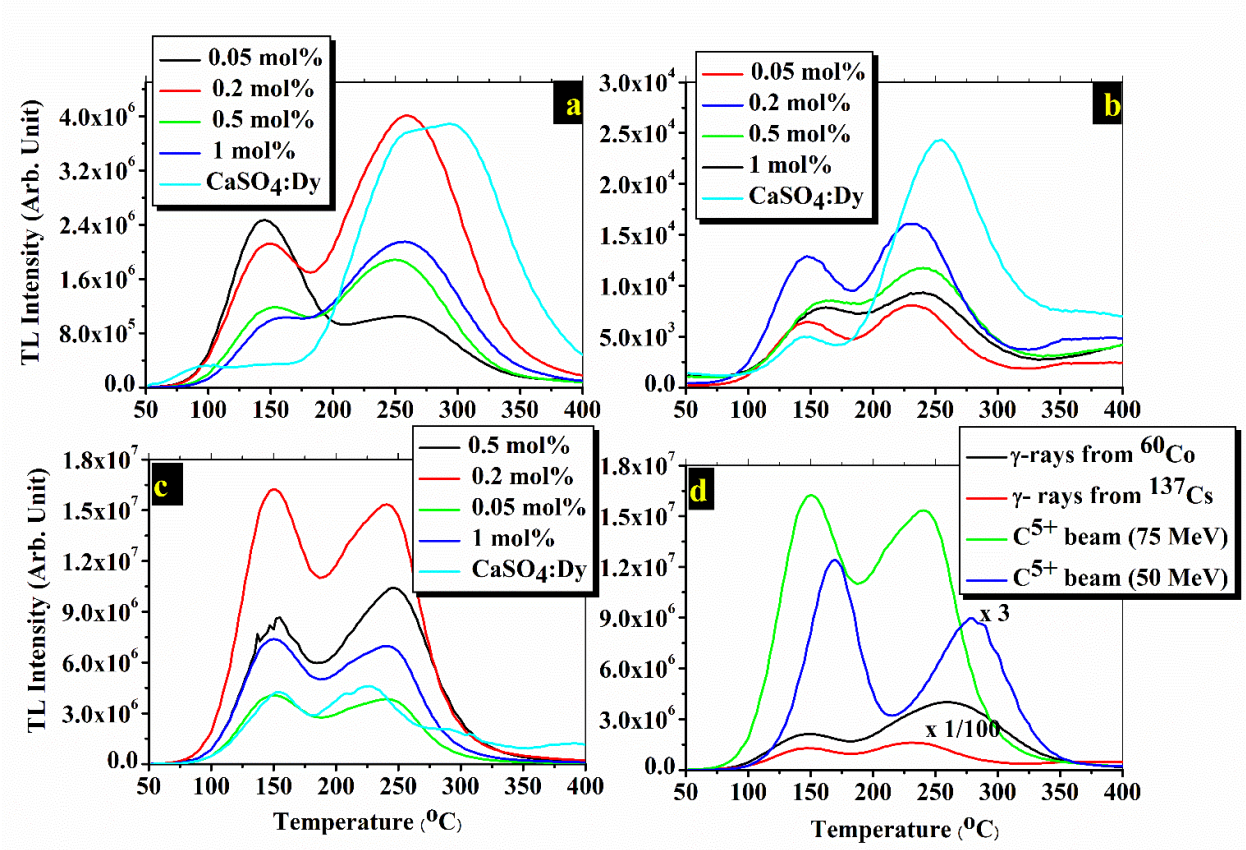

FIG. 4 TL glow curves of CMS phosphor irradiated with a) γ-rays from ^{60}Co source at 15Gy dose, b) γ-rays from ^{137}Cs source at 2300mRad dose, c) C^{5+} ion beam at 75MeV energy at 216kGy and (d) Comparison between TL glow curves of CMS phosphor irradiated with C^{5+} ion beam at 50, 75MeV energies and γ-rays from ^{60}Co source at 15 Gy dose and ^{137}Cs source at 2300mRad dose.

Thermoluminescence is a very common and simple technique used for estimation of doses of high-energy ionizing radiations absorbed by materials. In this work the TL study of this phosphor was carried out to propose its use in monitoring not only conventional radiation beams but also heavy ion beams such as carbon. The TL glow curves were recorded with the help of Harshaw TLD reader. For TL readout the fix mass (5mg) of irradiated sample was placed on a heating planchet which is then allowed to heat at the rate of 5°Cs^{-1}. The light coming out from the sample was detected by photomultiplier tube, which is placed perpendicular to the sample. Fig. 4(a) shows typical TL glow curves of CMS phosphor, irradiated with γ-rays from ^{60}Co source at 15Gy dose. The glow curve consists of good dosimetric peak at 260 °C with a small low temperature peak at 150°C. Among the four different concentrations of Dy^{3+}, maximum TL sensitivity was observed for 0.2mol%

concentration. For comparison of TL sensitivity we also took TL of standard TLD ($CaSO_4:Dy^{3+}$) phosphor. It was observed that the sensitivity of CMS phosphor is about 50% compared to the sensitivity of $CaSO_4:Dy^{3+}$. Fig. 4(b) shows the TL glow curve of CMS phosphor for γ-rays irradiation from ^{137}Cs source at 2300mRad. The glow curve shape of ^{137}Cs irradiated samples was found to be similar to ^{60}Co irradiated samples, but there is a shift in glow peak position towards lower temperature side when irradiated with ^{137}Cs source. The observed shift was about 3°C for peak 1 and about 28°C for peak 2. This shift is may be due to the alteration in the position of trapping levels inside forbidden band gap. As could be seen from Fig. 4 (c), the glow curve structures of CMS exposed to carbon ions (50 and 75MeV) are similar to that of γ-irradiated samples. The glow curves of CMS exposed to two different energies of carbon ion beams are qualitatively similar but quantitatively, there is a difference in glow peak temperature and relative intensities of glow peaks, which leads to the modifications in the trapping parameters. Various authors reported the significant variations in the glow curve structures and the positions, when samples are irradiated with different sources [22-24]. CMS phosphor was found to possess a stable glow curve which is stable with variation in irradiation species, as the carbon ion and γ-ray irradiated samples show 11 and 8% fading respectively, over 16 days of storage, see section F. In comparison to our phosphors the standard TLD phosphor $CaSO_4:Dy^{3+}$ shows significant change in the shape of the glow curve, when exposed to carbon ion beam. As could be seen in Fig. 4, the glow curve structure of CMS exposed to carbon ions at two different energies (i.e., 50 and 75MeV) is almost similar to that of γ-irradiated sample from ^{137}Cs and ^{60}Co sources. There is a small difference between the TL glow peak temperature for γ-irradiated sample from ^{60}Co and ^{137}Cs sources. In case of γ-irradiated samples using ^{60}Co source the second peak at 260°C is prominent than the lower temperature peak at 146°C when compared with TL glow curves of γ-irradiated samples using ^{137}Cs source. The lower temperature peak shows significant growth compared to high temperature peak. This clearly indicates that the number of traps responsible for these peaks is not in the same proportion, in the two cases. For 75MeV C^{5+} ion irradiated samples, there is formation of additional trapping levels which yields 2 more glow peaks compared to γ-ray irradiated samples. The occurrence of additional glow peaks at 185°C and 232°C suggest the formation of intermediate trapping levels in between the trapping levels responsible for occurrence of glow peak at 143°C and 242°C. Moreover, the C^{5+} ion irradiated samples (50MeV) show significant change in the position as well as intensity of the glow curve compared to glow curves of C^{5+} ion irradiated samples at 75MeV. The C^{5+} ion irradiation at 50MeV energy not only alters the positions of trapping levels

causing shift in the glow peak temperatures but also creates one additional trapping level which results in additional glow peak. On irradiating samples with C^{5+} ions there may be the formation of new trapping and luminescent centers, which are responsible for this anomalous behavior. Similar effects in the TL response of $CaSO_4:Dy^{3+}$ phosphor on C^{6+} ion beam irradiation has been reported by some authors [25]. It is expected that on irradiating samples with a relatively high energetic ion beams such as 50 and 75MeV C^{5+} ions, there will be changes in the TL glow curve structure, since the TL trapping and recombination mechanism are very sensitive to any perturbation. The variation is more when atomic displacements are due to non-elastic collisions and ionization due to secondary particles takes place [26]. The obtained results show that there is not much variation in the structure of the glow curve but there are minor changes in glow peak temperature, number of glow peaks, and TL intensity, which are responsible for variation in trapping parameters. These variations in trapping parameters are due to the disorganization of the initial localized energy levels in the mixed sulfate host as a result of high energy ion irradiation.

2. Dose response

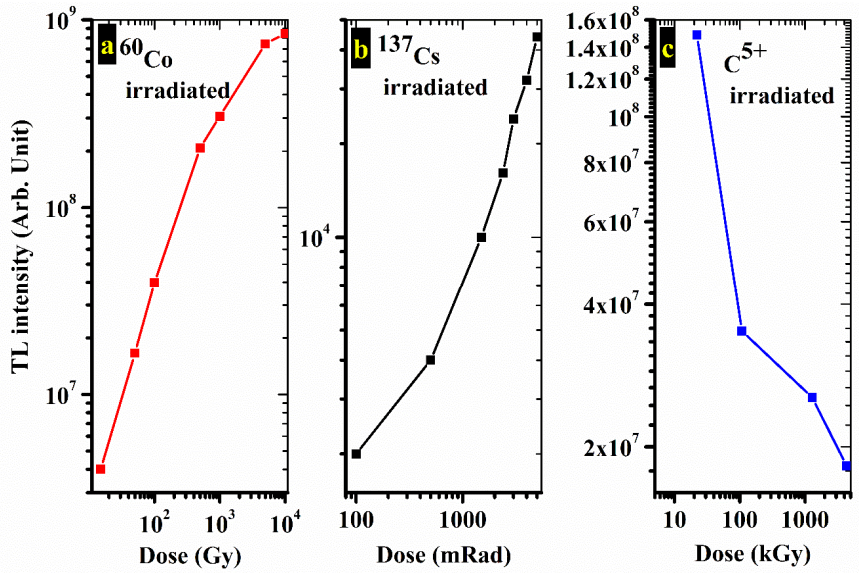

FIG. 5 The TL response curves of CMS phosphor irradiated by γ-rays from (a) ^{60}Co, (b) ^{137}Cs and (c) C^{5+} ion beam.

The TL response curves of CMS phosphor irradiated by γ-rays from ^{60}Co, ^{137}Cs sources and carbon ion beam is shown in Fig. 5 (a), (b) and (c) respectively. The TL response curve of the materials irradiated by γ-rays within a dose range 10Gy–10kGy shows linear response upto 1000Gy, above 1000Gy a slight saturation is observed. The phosphor irradiated with γ-rays

from ^{137}Cs source also shows linear response from 100mRad to 5Rad. Unlike γ-rays, the TL response of CMS phosphor towards carbon ion beam shows early saturation, when irradiated within dose range of 22kGy to 4MGy. The saturation in the TL response of CMS phosphor can be explained on the basis of track interaction model (TIM) [27,28]. The intensity of TL signal increases in proportion to the number of ion tracks. At higher fluences (due to large flux), the distance between nearest neighboring tracks decreases and probability of electrons escaping from the host track ion and reaching neighboring tracks increases. This results in increased luminescence recombination and ultimately increases the TL intensity. As the fluence increases further saturation effects occur, where the distances between nearby tracks decreases and the track begin to interact and overlap. These overlapping regions do not give additional TL, since they do not form additional trapping charge carriers due to the full occupancy of the available trap and luminescence centers. As the energetic ions are implanted in the matrix, they may be creating new kinds of defects, which make the process more complicated. The influence of 50, 75MeV carbon ion beams is definitely more than that of γ-rays and therefore the corresponding cross section of tracks of C^{5+} ions inside CMS phosphor is higher. The low linear energy transfer (LET) radiations such as γ-rays, electrons etc. give higher luminescence efficiency as compared to high LET radiations (heavily charged particles). However, these high LET radiations may induce additional defects in the host material as compared to low LET radiations and with increase in the radiation exposure the density of defects inside host increases leading to increase in peak intensity.

The dose delivered by carbon beam was calculated using equation (1)

$$D(\mathrm{Gy}) = 1.602\times10^{-10}\times\frac{\mathrm{dE/\,dX}}{\rho}(\mathrm{MeVcm^2/\,g})\times\phi(\mathrm{particles/\,cm^2}) \qquad \text{------(1)}$$

where dE/dx is the mean energy loss, ρ is the density of target material, and Φ is the ion fluence. The energy loss (linear energy transfer) was calculated using Monte Carlo simulation based TRIM code given by Ziegler *et al.*[29]. The maximum penetration depth inside material was calculated to be 89μm which is less than thickness of the pellet i.e. 0.075cm. The energy loss values for 50MeV and 75MeV are 2330 and 1760(MeV cm^2/g) respectively. These values are an indication of the amount of ionization caused by ions inside the target material. The values suggest that the ionization caused by 50MeV ion beam is higher than 75MeV beam. This also reflects in TL where higher sensitivity was observed for 50MeV irradiated sample. Moreover, the penetration depth for 50MeV and 75MeV energies was

calculated to be 48 and 89µm respectively. The present phosphor shows decrease in TL sensitivity after 23kGy dose of C^{5+} ion beam. This remarkable result is extremely important for CMS to be used as a dosimeter for such high doses of ion beams irradiation.

D. PL study

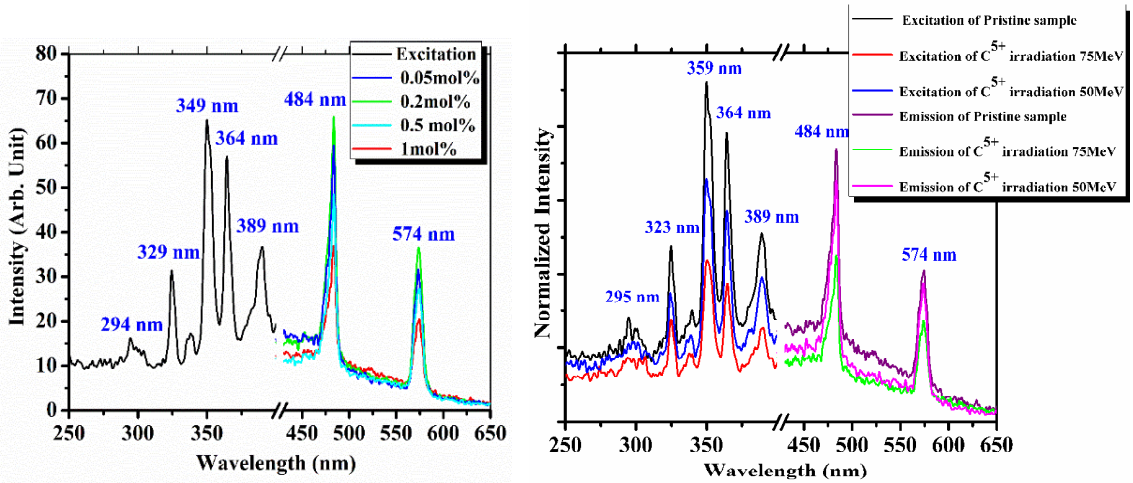

FIG. 6 (a) PL of CMS phosphor for different concentration of Dy^{3+}, (b) PL of carbon ion irradiated CMS (Dy^{3+}=0.2mol%) phosphor at 50 and 75MeV energy and pristine sample.

PL excitation and emission spectra for different mol% concentration of Dy^{3+} doped CMS pristine phosphor is shown in Fig. 6(a). The excitation spectrum of pristine CMS phosphor shows number of excitation peaks with prominent peak at around 349nm.The emission spectrum was recorded at this excitation wavelength shows characteristic emission peaks of Dy^{3+} at around 484nm and 574nm which are assigned to the transitions $^4F_{9/2} \rightarrow {}^6H_{15/2}$ and $^4F_{9/2} \rightarrow {}^6H_{13/2}$ respectively [30]. Fig. 6(b) shows the PL excitation and emission spectrum of 1mol% Dy^{3+} doped CMS phosphor irradiated with 50 and 75MeV carbon ion along with that of pristine phosphor. From the excitation and emission spectra it was observed that phosphor exposed with carbon ion beam show decrease in PL emission intensity and with further increase in energy of carbon ion beam, the emission intensity goes on decreasing. This decrease is possibly due to several reasons, 1) destruction of luminescence centers which are responsible for emission, 2) the irradiation induced residual absorption can absorb both, the excitation light as well as emission light, and 3) ion-induced defects can damage the microstructure of the phosphor [31].

At high ion fluences structural changes inside sample takes place which may reduce its PL output. This effect is directly influenced by the energy loss of the ions and thus by the

size and the damage concentration. The observed saturation in the TL glow curves and Dy^{3+} PL emissions of the samples exposed to 75MeV C^{5+} ions beam might be due to the more penetration depth of ion beam. But for 50MeV ion beam the penetration is less and the backscattering could be more, resulting in less number of implanted ions; therefore, it is still showing higher TL and PL efficiency.

E. Glow curve analysis

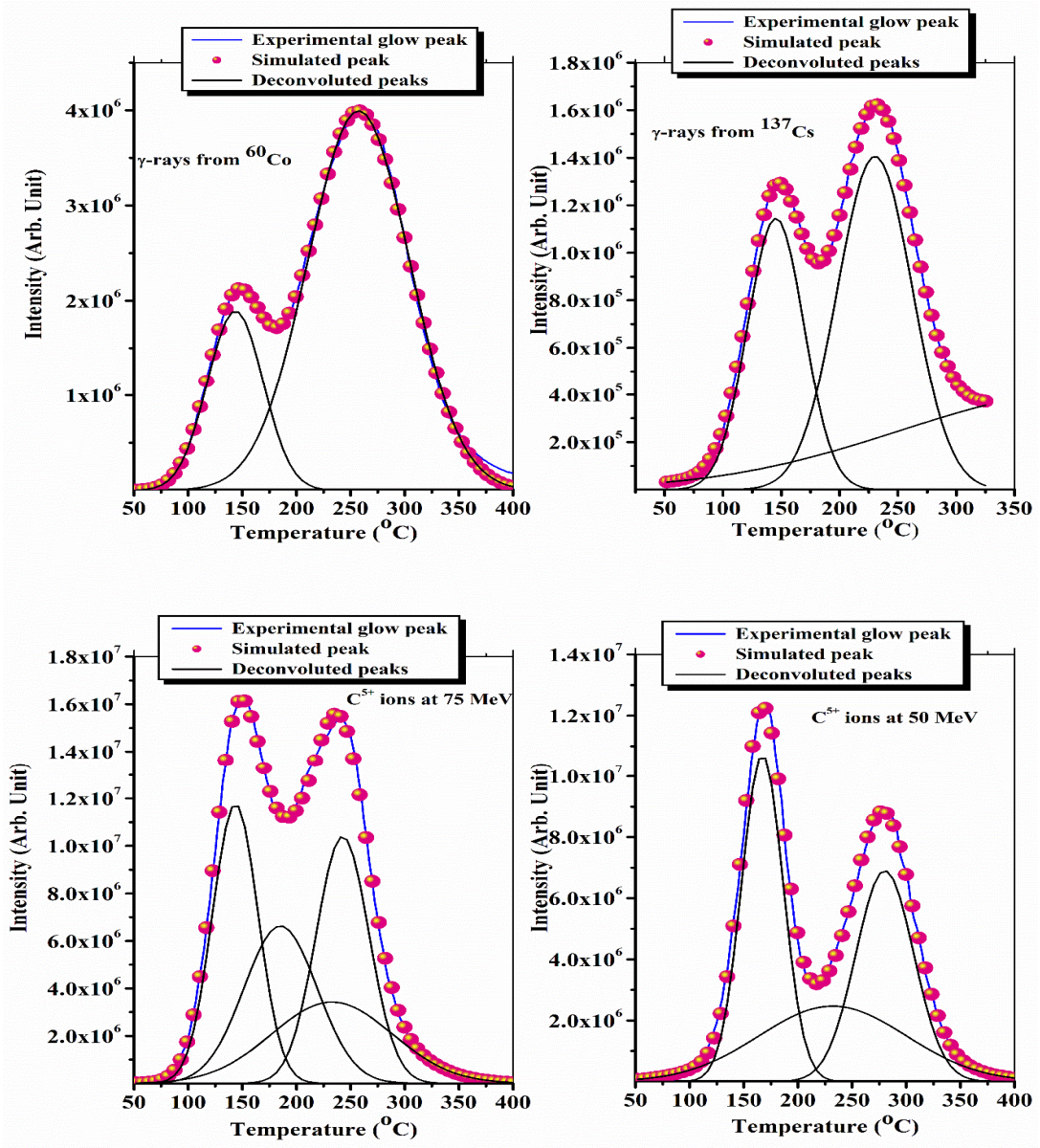

FIG.7 Comparison between the experimental (—), theoretically fitted(•) and deconvoluted (—) TL glow curves of CMS phosphor exposed to a) 15Gy of γ-rays from ^{60}Co, b) 2300mR

of γ-rays from ^{137}Cs, c) 216kGy of 75MeV C^{5+} ion beam, and d)108 kGy of 50MeV C^{5+} ion beam.

To verify further, the energy levels and other kinetic parameters of the glow peaks in all three cases, their glow curves deconvolution were done using GCD functions suggested by Kitis *et al*. [32].

For general order,

$$I = I_m b^{\left(\frac{b}{b-1}\right)} exp\left(\frac{E}{kT}\frac{T-T_m}{T_m}\right) \times \qquad \text{------ (2)}$$

$$\left[(b-1)\left(1-\frac{2kT}{E}\right)\frac{T^2}{T_m^2} exp\left(\frac{E}{kT}\frac{T-T_m}{T_m}\right) + 1 + (b-1)\frac{2kT_m}{E}\right]^{-(b/(b-1))}$$

where, I(T) is the TL intensity at temperature T (K), I_m- the maximum peak intensity, E- the activation energy (eV) and k- the Boltzmann constant.

They were applied to the experimentally obtained glow curves to isolate each peak. Firstly, the order of kinetics and activation energy of one of the peaks was found using Chen's set of empirical formulae [33].

The trap depth is calculated using the following equation, which is independent of order of kinetics:

$$\mathbf{E = c_\gamma\,(kT_m^2/\gamma) - b_\gamma\,(2kT_m)} \qquad \text{------- (3)}$$

Where, γ is τ, δ, or ω are the constants c_γ and b_γ for the three equations (τ, δ, or ω), k is the Boltzmann constant, T_m- maximum peak temperature.

The frequency factor (s)

$$\frac{\beta E}{kT_m^2} = s\,exp\left(\frac{-E}{kT_m}\right)[1 + (b-1)\Delta_m] \qquad \text{--------- (4)}$$

where, $\Delta_m = 2kT_m/E$, b is the order of kinetics, k is the Boltzmann constant and β is the linear heating rate (5 °Cs^{-1}).

To determine the order of kinetics (b); the form factor μ_g ($\mu_g=(T_2-T_m)/(T_2-T_1)$), which involves T_1 and T_2 (temperatures corresponding to half of the intensities on either side of the maximum) was calculated. This form factor μ_g is independent of the activation energy (E) and strongly depends on the order of kinetics (b). Finally the peak was generated theoretically using these parameters and separated from the main experimental glow curve. The benefit of

using GCD method is that most of the parameters used for generating a theoretical curve are easily derived from the experimentally recorded glow curve. The thermal activation energy (E) was again calculated using the same set of equations. This procedure was repeated for each TL peak till a good fit between experimental and theoretical glow curve was obtained.

Type of irradiation	Peak Number	T_m (°C)	μ_g	E (eV)	S (s^{-1})
	1	146	0.44	0.60	4.11×10^{6}
^{60}Co	2	258	0.48	0.61	9.07×10^{4}
	1	145	0.5	0.83	2.6×10^{9}
^{137}Cs	2	230	0.5	0.87	9.3×10^{7}
	1	143	0.5	0.93	5.5×10^{10}
C^{5+} 75MeV	2	185	0.5	0.67	4.44×10^{6}
	3	232	0.48	0.43	1.64×10^{3}
	4	242	0.5	1.21	2.3×10^{11}
	1	167	0.5	1.09	9.14×10^{11}
C^{5+} 50MeV	2	234	0.48	0.36	2.9×10^{2}
	3	280	0.49	1.25	6.51×10^{10}

Table 1. Trapping parameters of CMS phosphor for different irradiations calculated by Chen's method.

The deconvolution of experimentally obtained glow peaks was carried out using glow curve deconvolution program. Deconvolution of experimental glow curves was carried out in order to show the number of individual glow peaks present in complex glow curve, as shown in Fig. 7. The isolated glow peaks were then examined for gathering the information about trapping parameters. The generation of new absorption peaks with increase in energy of carbon ion beam also illustrates the change position of trapping levels, see Table 1.

F. Fading study

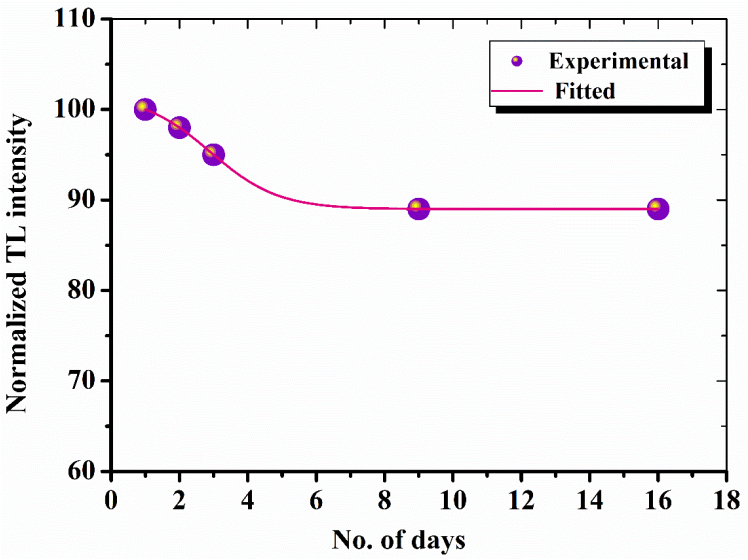

FIG. 8 Fading data of CMS sample.

For the fading study the γ-ray and carbon ion irradiated samples were stored for a few days without taking any precautions to shield it from light and moisture and the glow curves were recorded for a period of around 16 days, as shown in Fig. 8. Figure show the fading plot of gamma and carbon ion irradiated phosphor. It was observed that the higher temperature glow peak is quite stable against storage time. The carbon ion and γ-ray irradiated samples show 11 and 8% fading respectively, over 16 days of storage.

G. Absorption spectra

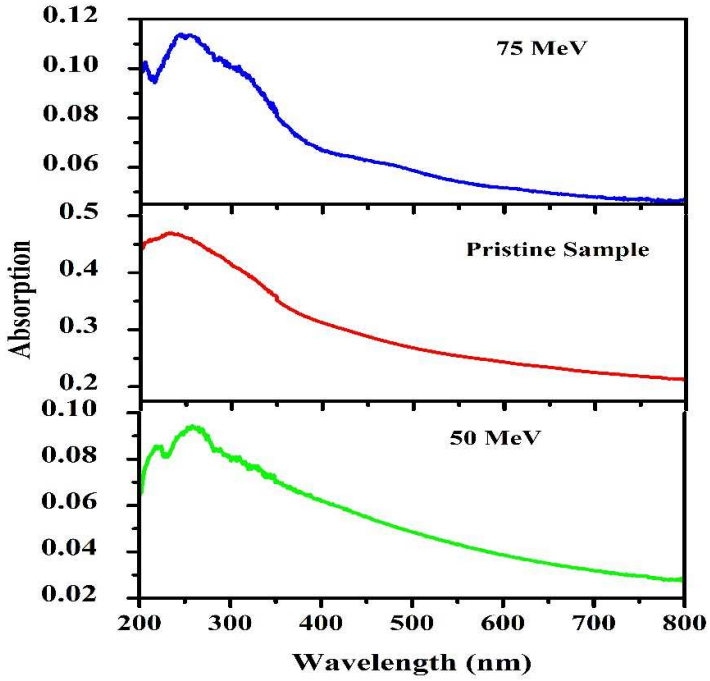

FIG. 9 Absorption spectra of CMS sample.

Fig. 9 shows the absorption spectra of CMS phosphor, for 0.2mol% Dy^{3+} doping. The calculated band gap energy of pristine sample is 5.34eV. It has been observed that the absorption of the phosphor increases with increase in energy of the ion beam. This increase is due to generation of large number of defects at these energies of ion beam. The absorption was found to be shifted towards higher wavelength side with increase in beam energy. The difference between band gap energy and energy of absorption peak represent the activation energy of trapped charge carriers. The sample irradiated by 50MeV ion beam have absorption at 219, 258, 317nm corresponding to 5.66, 4.80, 3.911eV energies and by 75MeV ion beam have absorption at 204, 243, 254, 313, 459nm corresponding to 6.07, 5.10, 4.88, 3.96, 2.70eV energies. The activation energies calculated from absorption spectra are nearly same as calculated by Chen's peak shape method.

IV. CONCLUSION

In conclusion we provide insight for synthesizing a CMS phosphor by acid distillation method with remarkable TL properties. The phosphor was found to be 3.5 times more sensitive than standard $CaSO_4:Dy^{3+}$ phosphor with stable dosimetric peak for C^{5+} ion irradiation. The TL response is nearly same for different types of irradiations. The irradiation

results in slight variation in glow peak position and ion beam irradiation causes additional glow peaks this influence the trapping parameters which is discussed in detailed. The obtained results can be easily correlated with physical phenomenon which suggests the usefulness of this phosphor for carbon ion beam dosimetry along with γ-ray dosimetry over a wide range of exposure.

Acknowledgement

Authors are grateful to Board of Research in Nuclear Sciences (BRNS), Department of atomic Energy, Govt. of India, for providing financial assistance to carry out this work under research project (sanctioned letter no 2011/37P/10/BRNS/144). The authors would like to thank the Director of the Inter-University Accelerator Centre (IUAC), New Delhi, for providing beam time. Authors are also grateful to the Director of Center for Advanced Technology, Indore, for providing ADXRD measurement facility and Dr. A.K Sinha and Dr. M.N Singh for their support during ADXRD measurement.

1. W. Barth, L. Dahl, J. Glatz, P. Forck, J. Klabunde, Proceedings of the Particle Accelerator Conference, Chicago, 3281 (2001).
2. W. Barth, L. Dahl, J. Glatz, L. Groening, S. Richter, S. Yaramishev, Proceedings DIPAC, 161 (2003).
3. Th. Haberer, AIP Conf. Proc., 610 (2002) 157.
4. H. Eickhoff, T. Haberer, G. Kraft, U. Krause, M. Richter, R. Steiner, J. Debus, Strahlenther Onkol, 175 (1999) 21.
5. U. Amaldi, G. Kraft, Rep. Prog. Phys.68 (2005) 1861–1882.
6. H. Tsujii, J. Mizoe, T. Kamada, M. Baba, H. Tsuji, H. Kato, S. Kato, S. Yamada, S. Yasuda, T. Ohno, T. Yanagi, R. Imai, K. Kagei, H. Kato, R. Hara, A. Hasegawa, M. Nakajima, N. Sugane, N. Tamaki, R. Takagi, S. Kandatsu, K. Yoshikawa, R. Kishimoto, T. Miyamoto, J. Radiat. Res., 48 (2007) 1-13.
7. H. Tsujii, T. Kamada, M.i Baba, H. Tsuji, H. Kato, S. Kato, S. Yamada, S. Yasuda, T. Yanagi, H. Kato, R. Hara, N. Yamamoto, J. Mizoe, New J. Phys 10 (2008) 075009.
8. G. Kraft, Nucl. Instr. and Meth.A, 454 (2000) 1.
9. J. Heilmann, G. Taucher-Scholz, T. Haberer, M. Scholz, G. Kraft, Int. J. Radiat. Oncol.Biol.Phys.34 (1996) 599.
10. P.D. Sahare, S.V. Moharil, J. Phys. D: Appl. Phys. 23 (1990) 567.

11. A. Pandey, P.D. Sahare, J.S. Bakare, S.P. Lochab, F. Singh, D. Kanjilal, J. Phys. D: Appl. Phys. 36 (2003) 2400.
12. B.P. Kore, N.S. Dhoble, K. Park, S.J. Dhoble, J. Lumin. 143 (2013) 337.
13. S.J. Dhoble, S.V. Moharil, T.K. Gundu Rao, J. Lumin. 93 (2001) 43.
14. T. Berger, G. Reitz, M. Hajek, N. Vana, Adv. in Space Res.37 (2006) 1716.
15. T. Yamashita, N. Nada, H. Onishi, S. Kitamura, Health Phys. 21 (1971) 295.
16. D. Kanjilal, S. Chopra, M.M. Narayanan, Indira S. Iyer, Vandana Jha, R. Joshi, S.K. Datta, Nucl. Instr. and Meth. A 328 (1993) 97.
17. S.R. Kane, C.K. Garg, A.K. Sinha, AIP Conf. Proc. 1234 (2010) 689.
18. A.K. Sinha, A. Sagdeo, P. Gupta, A. Kumar, M.N. Singh, R.K. Gupta, S.R. Kane, and S.K. Deb, AIP Conf. Proc.1349 (2011) 503.
19. A.P. Hammersley, ESRF Internal Report ESRF98HA01T, FIT2D V9.129 Reference Manual V3.1, 1998.
20. See supplemental material at [URL will be inserted by RSC].
21. J. Manam, S. Das, J.Alloy Compd. 489 (2010) 84.
22. P.D. Sahare, N. Salah, S.P. Lochab, T. Mohanty, D. Kanjilal, J. Phys. D: Appl. Phys. 38 (2005) 3995.
23. B. Yang, L. Xie, Y.Xu, P.D. Townsend, Nucl. Instr. and Meth.in Phys. Res. B 187 (2002) 408.
24. A.T. Davidson, A.G. Kozakiewicz, D.J. Wilkinson, J.D. Comins, T.E. Derry, Nucl. Instr. and Meth.in Phys. Res. B141 (1998) 523.
25. N. Salah, J. Phys. D: Appl. Phys. 41 (2008) 155302.
26. O.B. Geiß, M. Krämer, G. Kraft, Nucl. Instr.And Meth.in Phys. Res. B, 142, 592 (1998).
27. Y.S. Horowitz, D. Satinger, L. Oster, N. Issa, M.E. Brandan, O. Avila, M. Rodriguez-Villafuerte, I. Gamboa-deBuen, A.E. Buenfil, C. Ruiz-Trejo, Radiat. Meas., 33 (2001) 459.
28. Y.S. Horowitz, O. Avila, M. Rodriguez-Villafuerte, Nucl. Instr. and Meth. in Phys. Res. B, 184 (2001) 85.
29. J.F. Ziegler, J.P. Biersack, U. Littmark, The Stopping and Range of Ions in Solid, 1985.
30. B.P. Kore, N.S. Dhoble, S.P. Lochab, S.J. Dhoble, J. Lumin. 145 (2014) 299.
31. M. Batentschuka, A. Winnacker, K. Schwartz, C. Trautmann, J. Lumin. 125 (2007) 40
32. G. Kitis, J M Gomez-Ros, JWN Tuyn, J. Phys. D: Appl. Phys. 31 (1998) 2636
33. R. Chen, J. Electrochem. Soc.: Solid state Sciences, 116 (1969) 1254.